

# $U(1)_{L_\mu-L_\tau}$ for Light Dark Matter, $g_\mu - 2$ , the 511 keV excess and the Hubble Tension

---

Manuel Drees<sup>a</sup> Wenbin Zhao<sup>a</sup>

<sup>a</sup>*Bethe Center for Theoretical Physics and Physikalisches Institut, Universität Bonn  
Nussallee 12, 53115 Bonn, Germany*

*E-mail:* [drees@th.physik.uni-bonn.de](mailto:drees@th.physik.uni-bonn.de), [wenbin.zhao@uni-bonn.de](mailto:wenbin.zhao@uni-bonn.de)

**ABSTRACT:** In this paper we introduce a light Dirac particle  $\psi$  as thermal dark matter candidate in a  $U(1)_{L_\mu-L_\tau}$  model. Together with the new gauge boson  $X$ , we find a possible parameter space with  $m_X \simeq 20$  MeV,  $U(1)_{L_\mu-L_\tau}$  coupling  $g_X \simeq 5 \cdot 10^{-4}$  and  $m_\psi \gtrsim m_X/2$  where the  $(g-2)_\mu$  anomaly, dark matter, the Hubble tension, and (part of) the excess of 511 keV photons from the region near the galactic center can be explained simultaneously. This model is safe from current experimental and astrophysical constraints, but can be probed by the next generation of neutrino experiments as well as low-energy  $e^+e^-$  colliders.

---

## Contents

<b>1</b>	<b>Introduction</b>	<b>1</b>
<b>2</b>	<b>The Model</b>	<b>2</b>
<b>3</b>	<b>Constraints</b>	<b>3</b>
3.1	Dark Matter Relic Density	4
3.2	Direct Dark Matter Detection	6
3.3	Big Bang Nucleosynthesis and Hubble Tension	6
3.4	Cosmic Microwave Background	8
3.5	White Dwarf Cooling	9
3.6	Other Experimental Constraints	10
3.6.1	Neutrino Trident Production	10
3.6.2	Coherent Elastic Neutrino Nucleus Scattering	10
3.6.3	$X$ Production at BaBar	10
3.7	Summary of the Allowed Parameter Space	10
<b>4</b>	<b>511keV Line</b>	<b>11</b>
<b>5</b>	<b>Future Tests</b>	<b>14</b>
<b>6</b>	<b>Summary and Conclusions</b>	<b>14</b>

---

## 1 Introduction

The  $U(1)_{L_\mu-L_\tau}$  model [1] is a well-motivated extension of the Standard Model (SM). It contains a new gauge boson which couples to second and third generation leptons. The model is free of anomalies with SM particle content; this remains true in the presence of right-handed SM singlet neutrinos, if two of them carry equal but opposite  $U(1)_{L_\mu-L_\tau}$  charges of  $\pm 1$ . Moreover, it allows to explain [2, 3] the  $4.2\sigma$  discrepancy between the recent measurement of the muon’s anomalous magnetic moment [4] and SM predictions [5].

The new gauge boson can also serve as a mediator between SM particles and cosmological dark matter (DM) [2]. Thus this model has been used to study dark matter physics in the GeV to TeV range by introducing spinor or scalar DM, as possible weakly interacting massive particle (WIMP) candidates [6–9]. It can produce the correct thermal relic density in minimal cosmology without violating existing DM search bounds. However, in this mass range a relatively large  $U(1)_{L_\mu-L_\tau}$  coupling  $g_X$  is required, which leads to a host of constraints [10, 11].

The experimental constraints from direct DM searches are considerably weaker in the MeV range. Moreover, the explanation of  $g_\mu - 2$  now requires a gauge coupling below

$10^{-3}$ . Previous studies showed that near-resonant DM annihilation, co-annihilation, or a DM charge  $\gg 1$  is needed in order to reproduce the DM relic abundance in this region of parameter space [12–16].

For DM and gauge boson masses below the muon mass the dark sector couples primarily to neutrinos. The decoupling of DM particles, and the decay of the gauge bosons, can therefore increase the energy density in neutrinos, corresponding to a change  $\delta N_{\text{eff}} \lesssim 0.4$  [17], which relaxes the tension between cosmological and “local” measurements of the Hubble constant [18, 19].

As already mentioned, the DM mass  $m_\psi$  needs to be close to  $m_X/2$  in order to reproduce the thermal relic density in minimal cosmology. If  $m_\psi < m_X/2$  the thermally averaged DM annihilation cross section  $\langle\sigma v\rangle$  will fall after DM decoupling, making DM annihilation in today’s Universe essentially unobservable. On the other hand, if  $m_\psi > m_X/2$ ,  $\langle\sigma v\rangle$  will increase after DM decoupled. In this case annihilation into  $e^+e^-$  pairs, which is possible due to kinetic mixing between the new gauge boson and the photon, can even (help to) explain the excess of 511 keV photons from the region around the center of our galaxy that has been observed since the 1970’s [20–24].

The remainder of this paper is organized as follows. In Sec. 2 we introduce the model Lagrangian and discuss some relevant phenomenology. In Sec. 3 we discuss important constraints on the new gauge boson and DM particles from several different experiments and observations. In Sec. 4 we apply our model to the 511 keV line, while Sec. 5 briefly discusses future tests of the model. Finally, Sec. 6 contains a brief summary and some conclusions.

## 2 The Model

Our model is based on an  $SU(3)_c \times SU(2)_L \times U(1)_Y \times U(1)_{L_\mu-L_\tau}$  gauge theory. In addition to the well-known SM particles, we introduce an SM singlet Dirac DM  $\psi$  with  $U(1)_{L_\mu-L_\tau}$  charge  $q_\psi$  and a spin 1 gauge boson  $X$ . The  $\mu$  and  $\tau$  family leptons are assigned charge 1 and  $-1$ , respectively. Since the Dirac DM particle  $\psi$  contains two two-component spinors with opposite  $U(1)_{L_\mu-L_\tau}$  charges, the model remains anomaly-free for any value of  $q_\psi$ .

The  $U(1)_{L_\mu-L_\tau}$  model can also have a rich neutrino phenomenology [25–27]. We will assume that the right-handed, SM singlet neutrinos needed to generate realistic neutrino masses have masses well above  $m_\psi$ , in which case they play no significant role in the phenomena studied in this paper. Moreover, the Higgs boson needed to break  $U(1)_{L_\mu-L_\tau}$  cannot couple to  $\psi$  directly and thus also plays no role in the phenomenology we are interested in. The relevant part of the Lagrangian of our model thus reads:

$$\begin{aligned} \mathcal{L} = \mathcal{L}_{SM} &- g_X X_\lambda (\bar{\mu} \gamma^\lambda \mu - \bar{\tau} \gamma^\lambda \tau + \bar{\nu}_{\mu L} \gamma^\lambda \nu_{\mu L} - \bar{\nu}_{\tau L} \gamma^\lambda \nu_{\tau L}) \\ &- \frac{1}{4} X_{\mu\nu} X^{\mu\nu} + \frac{1}{2} m_X^2 X_\mu X^\mu \\ &+ \bar{\psi} (i \not{D} - m_\psi) \psi - q_\psi g_X X_\lambda \bar{\psi} \gamma^\lambda \psi. \end{aligned} \quad (2.1)$$

Here  $g_X$  is the  $U(1)_{L_\mu-L_\tau}$  gauge coupling,  $X_{\mu\nu} = \partial_\mu X_\nu - \partial_\nu X_\mu$  is the  $U(1)_{L_\mu-L_\tau}$  field strength tensor and  $m_X$  is the mass of the new gauge boson.

Note that we assume the  $U(1)_{L_\mu-L_\tau}$  group to be orthogonal to the SM gauge group; in particular, there is no tree-level kinetic mixing between the two  $U(1)$  factors. However, once the vacuum expectation value of the SM Higgs boson is taken into account, so that the charged leptons obtain masses, this mixing is induced radiatively through loops involving  $\mu$  and  $\tau$  leptons. This mixing adds an additional interaction term:

$$\begin{aligned}\mathcal{L}_{X,J_{\text{em}}} &= -\epsilon_A e X_\mu J_{\text{em}}^\mu, \\ \epsilon_A &= -\frac{eg_X}{12\pi^2} \ln\left(\frac{m_\tau^2}{m_\mu^2}\right) \approx -\frac{g_X}{70},\end{aligned}\tag{2.2}$$

where  $J_{\text{em}}^\mu$  is the electromagnetic current. The mixing between  $X$  and the SM  $Z$  boson is further suppressed by  $\frac{m_X^2}{m_Z^2}$ ; it is thus completely negligible for  $m_X \lesssim 100$  MeV, which is the range of masses we are interested in.

Important processes which determine dark matter phenomenon are  $\psi\bar{\psi} \rightarrow f\bar{f}$  annihilation, where  $f$  are SM particles with coupling to the  $X$  boson. The corresponding cross section reads:

$$\sigma(s) = \frac{g_X^4 q_\psi^2}{12\pi} \sqrt{\frac{s - 4m_f^2}{s - 4m_\psi^2}} \frac{s^2 + 2(m_\psi^2 + m_f^2)s + 4m_f^2 m_\psi^2}{s[(s - m_X^2)^2 + \Gamma_X^2 m_X^2]}.\tag{2.3}$$

Here  $\Gamma_X$  is the total width of the  $X$  boson. It is the sum of the partial widths:

$$\begin{aligned}\Gamma(X \rightarrow l^+ l^-) &= \frac{g_X^2 m_X}{12\pi} \left(1 + \frac{2m_l^2}{m_X^2}\right) \sqrt{1 - \frac{4m_l^2}{m_X^2}}, \\ \Gamma(X \rightarrow \bar{\nu}_l \nu_l) &= \frac{g_X^2 m_X}{24\pi},\end{aligned}\tag{2.4}$$

where  $l = \mu$  or  $\tau$ .

Recently the Fermilab Muon  $g - 2$  Experiment has published their first results, which confirmed a positive deviation from the SM prediction [4]. Together with older results from the BNL E821 experiment [28], the measurements exceed the SM prediction [5] by  $4.2\sigma$ :

$$\Delta\alpha_\mu = \alpha_\mu(\text{Exp}) - \alpha_\mu(\text{SM}) = (251 \pm 59) \times 10^{-11},\tag{2.5}$$

which is a quite strong hint for BSM physics. Our model contributes to  $(g-2)_\mu$  at one-loop level [2, 3]:

$$\Delta\alpha_\mu = \frac{g_X^2}{8\pi^2} \int_0^1 dx \frac{2m_\mu^2 x^2 (1-x)}{x^2 m_\mu^2 + (1-x)m_X^2}.\tag{2.6}$$

This reproduces the measurement (2.5) for  $g_X \simeq 4.4 \cdot 10^{-4}$  if  $m_X^2 \ll m_\mu^2$ , and for  $g_X \simeq 5.4 \cdot 10^{-4} m_X/m_\mu$  if  $m_X^2 \gg m_\mu^2$ .

### 3 Constraints

In this section we discuss the most relevant constraints on the parameter space. We focus on cosmological and astrophysical constraints; other constraints are briefly summarized in the last subsection.

### 3.1 Dark Matter Relic Density

We want  $\psi$  to have the correct thermal relic density in standard cosmology. We compute the relic density by approximately solving the Boltzmann equation using the formalism established in [29]:<sup>1</sup>

$$\frac{dn_\psi}{dt} + 3Hn_\psi = -\frac{\langle\sigma v\rangle}{2}(n_\psi^2 - n_{\psi,eq}^2). \quad (3.1)$$

We assume equal  $\psi$  and  $\bar{\psi}$  density; the factor 1/2 appears since only  $\psi\bar{\psi}$  encounters can lead to annihilation, while  $\psi\psi$  and  $\bar{\psi}\bar{\psi}$  encounters cannot. For  $m_\psi < m_\mu$  the most relevant annihilation process is  $\psi\bar{\psi} \rightarrow \nu_{\mu,\tau}\bar{\nu}_{\mu,\tau}$  mediated by  $X$  boson exchange in the  $s$ -channel. The corresponding thermally averaged cross section is [31]:

$$\langle\sigma v\rangle = \frac{1}{8m_\psi^4 T K_2^2(m_\psi/T)} \int_{4m_\psi^2}^{\infty} ds \sigma(s) \sqrt{s} (s - 4m_\psi^2) K_1\left(\frac{\sqrt{s}}{T}\right), \quad (3.2)$$

where the  $K_n$  are modified Bessel functions of order  $n$  and the annihilation cross section  $\sigma(s)$  is given by eq.(2.3) with  $m_f = 0$ . The scaled inverse decoupling temperature  $x_f = \frac{m_\psi}{T_f}$  is determined by solving the following equation iteratively:

$$x_f = \ln \frac{0.076 M_{\text{Pl}} m_\psi \langle\sigma v\rangle}{g_*^{1/2} x_f^{1/2}}. \quad (3.3)$$

Here  $M_{\text{Pl}} = 1.22 \cdot 10^{19}$  GeV is the Planck mass and  $g_*$  is the total number of effectively relativistic degrees of freedom at the time of freeze-out.

In order to compute the integral in eq.(3.2) reliably and with acceptable numerical effort, we split the integral in up to three regions. Well below and well above the resonance we use the original form of eq.(3.2), but for  $s \sim m_X^2$  we perform a change of variable:

$$y(s) = \arctan\left(\frac{s - m_X^2}{m_X \Gamma_X}\right). \quad (3.4)$$

It has been designed such that the Jacobian  $ds/dy$  removes the denominator in eq.(3.2), so that we have to compute the integral

$$I = \int_{y_-}^{y_+} \frac{s(s + 2m_\psi^2)}{m_X \Gamma_X} \sqrt{s - 4m_\psi^2} K_1\left(\frac{\sqrt{s}}{T}\right) dy. \quad (3.5)$$

The integration boundaries in eq.(3.5) are given by

$$\begin{aligned} y_- &= y(\max(0.9m_X^2, 4m_\psi^2)); \\ y_+ &= y(1.1m_X^2), \end{aligned} \quad (3.6)$$

where the argument of  $y$  should be inserted in eq.(3.4). Of course, for  $4m_\psi^2 > 1.1m_X^2$  this is not necessary since  $s$  always lies well above the resonance.

---

<sup>1</sup>We note in passing that MadDM [30] showed serious numerical instabilities in parts of the parameter space with  $m_\psi < m_X/2$ .

Before freeze-out dark matter is assumed to be in full kinetic and chemical equilibrium, while for  $T < T_f$ , i.e.  $x > x_f$ , DM annihilation dominates and reduces the dark matter abundance. This effect is described by the annihilation integral

$$J = \int_{x_f}^{\infty} \frac{\langle \sigma v \rangle}{x^2} dx. \quad (3.7)$$

The present day relic density is then given by:

$$\Omega_{\psi} h^2 = \frac{1.07 \cdot 10^9 \text{GeV}^{-1}}{J g_* M_{\text{Pl}}}. \quad (3.8)$$

Here  $\Omega_{\psi}$  is the mass density in DM particles (both  $\psi$  and  $\bar{\psi}$ ) in units of the critical density, and  $h$  is the scaled Hubble constant. Cosmological measurements imply  $\Omega_{\text{DM}} h^2 \simeq 0.12$  [32].

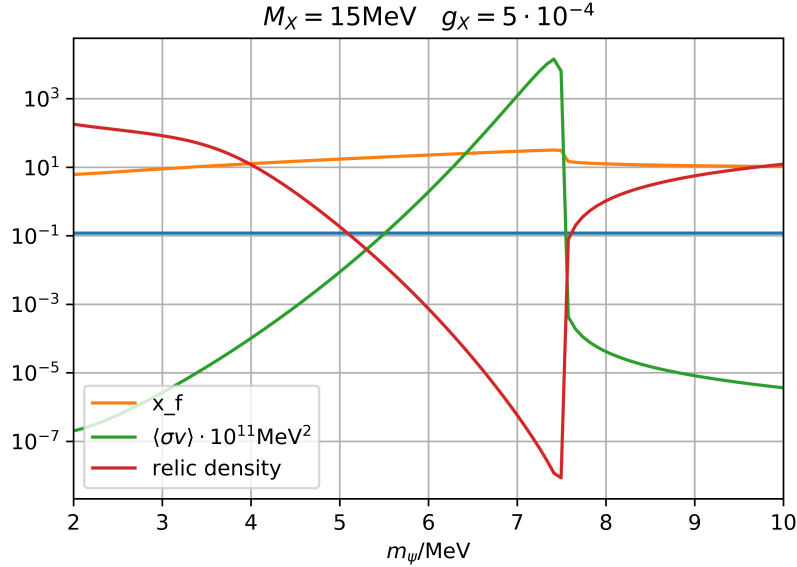


**Figure 1.** The predicted relic density (red), the thermal average of the annihilation cross section at decoupling (green) and the scaled inverse decoupling temperature  $x_f$  (orange) as function of the DM mass  $m_{\psi}$ , for  $m_X = 15$  MeV and gauge coupling  $g_X = 5 \cdot 10^{-4}$ . The blue line, representing  $\Omega h^2 = 0.12$ , is the desired dark matter relic density.

An example of the dependence of the relic density, and related quantities, on the DM mass  $m_{\psi}$  is shown in fig. 1. We see that the relic density, shown in red, decreases quickly as  $m_{\psi}$  approaches  $m_X/2$  from below. This is mirrored by the rise of the thermally averaged annihilation cross section at  $x = x_f$  (shown in green), and by the much slower rise of  $x_f$  (shown in orange) which depends on  $\langle \sigma v \rangle$  only logarithmically. At  $m_{\psi} = m_X/2$  the relic density shoots up by several orders of magnitude, and then continues to rise more slowly for yet larger DM masses. This asymmetry can be explained by the fact that for  $m_{\psi} < m_X/2$  the resonance  $s = m_X^2$  can always be reached for some kinetic energy of the DM particles; however, once  $m_{\psi} > m_X/2$  the resonance can no longer be accessed.

For the given parameters, which allow to explain the measurement of  $g_\mu - 2$ , the minimum of the predicted relic density, reached for  $m_\psi$  just below  $m_X/2$ , is several orders of magnitude below the desired value of 0.12, shown in blue. Hence the correct relic density can be obtained for two values of the DM mass, one about 30% below  $m_X/2$  and the other about 1.2% above  $m_X/2$ . It should be noted that for the solution with  $m_\psi < m_X/2$  the thermally averaged annihilation cross section will decrease at temperatures below  $T_f$ , since reduced average kinetic energy means that  $\sqrt{s}$  is usually further away from the pole; for this solution today's annihilation cross section, which (for galaxies like our own) should be computed at  $x \sim 10^{-6}$ , is considerably smaller than  $\langle\sigma v\rangle$  shown in fig. 1. In contrast, if  $m_\psi > m_X/2$  reducing the kinetic energy moves the  $\psi\bar{\psi}$  system closer to the pole, so that today's value of  $\langle\sigma v\rangle$  significantly exceeds that shown in fig. 1. We will come back to this point in Sec. 4.

### 3.2 Direct Dark Matter Detection

For  $m_\psi \ll 1$  GeV the most sensitive constraints come from DM–electron scattering. In our model the relevant interaction is described by the Lagrangian (2.2), leading to a scattering cross section of [33]:

$$\sigma(\psi e \rightarrow \psi e) = \frac{\mu_e^2}{\pi} \frac{\epsilon_A^2 e^2 q_\psi^2 g_X^2}{(m_X^2 + \alpha^2 m_e^2)^2}, \quad \mu_e = \frac{m_\psi m_e}{m_\psi + m_e}. \quad (3.9)$$

Several experiments have set upper bounds on this cross section: XENON10 [34], XENON1T [35], DarkSide50 [36] and SENSEI [37]. For a  $m_\psi \simeq 10$  MeV, the best current bound,  $\sigma(\psi e \rightarrow \psi e) \leq 0.5 \times 10^{-36} \text{ cm}^2$ , comes from the SENSEI experiment. On the other hand, for  $m_\psi \gg m_e$  (i.e.  $\mu_e \simeq m_e$ ),  $m_X^2 \gg m_e^2$  and  $\epsilon_A \simeq -g_X/70$ , eq.(3.9) yields

$$\sigma(\psi e \rightarrow \psi e) \simeq 6 \cdot 10^{-44} \text{ cm}^2 \left( \frac{g_X}{10^{-3}} \right)^4 \left( \frac{10 \text{ MeV}}{m_X} \right)^4 q_\psi^2. \quad (3.10)$$

For the parameter range of interest to us this is well below the present and near–future sensitivity

### 3.3 Big Bang Nucleosynthesis and Hubble Tension

Both our dark matter candidate  $\psi$  and the new gauge boson  $X$  couple to neutrinos. If their masses are well below the muon mass they will therefore dump their energy and their entropy into neutrinos. If this happens after neutrinos decouple from photons they will deliver extra entropy and energy exclusively into neutrinos, which would modify the history of Big Bang Nucleosynthesis (BBN) by speeding up the expansion rate of the universe. This effect has been well studied for the  $X$  boson [17, 38] and for DM particles [39] separately. Once again, we assume that both  $X$  and  $\psi$  were in full thermal equilibrium with the SM plasma at sufficiently high temperature; moreover, we assume that the initial temperature was above  $m_X$ , so that the initial  $X$  and  $\psi/\bar{\psi}$  densities were comparable to those of all other relativistic species. They then decay or annihilate into neutrinos when they become non–relativistic.

The impact on the neutrino energy density is usually parameterized by  $N_{\text{eff}}$ , defined by the total relativistic energy density well after electron–positron annihilation:

$$\rho_{\text{rad}} = \left[ 1 + N_{\text{eff}} \frac{7}{8} \left( \frac{4}{11} \right)^{\frac{4}{3}} \right] \rho_{\gamma}, \quad (3.11)$$

where  $\rho_{\gamma}$  is the energy density in photons. We compute  $N_{\text{eff}}$  using entropy conservation, rather than solving the Boltzmann equation. We make the following assumptions:

1. No chemical potential, i.e. no particle–antiparticle asymmetry in the neutrinos<sup>2</sup> or the  $\psi - \bar{\psi}$  sector.
2. The masses of new particles are much larger than the recombination temperature  $T_r \sim 1$  eV. For temperatures  $\lesssim T_r$  the  $X$  particles will then practically all have decayed away, while the DM particles are totally non–relativistic and do not contribute to the entropy anymore. Of course, contributions to  $N_{\text{eff}}$  from  $X$  decays and  $\psi\bar{\psi}$  annihilation after neutrino decoupling still persist.
3. We assume that all neutrinos decouple at the common temperature  $T_{\nu,D} = 2.3$  MeV. This is the decoupling temperature for  $\nu_{\mu}$  and  $\nu_{\tau}$  in the SM. Since  $X$  does not couple to electron neutrinos, and the  $X$  exchange contribution to the interactions between neutrinos and electrons or nuclei is subdominant (see below), this should be a good approximation. For  $T < T_{\nu,D}$  the neutrinos,  $X$ ,  $\psi$  and  $\bar{\psi}$  thus form a system that is decoupled from the photons.

The contributions from dark matter annihilation and  $X$  boson decay are then [40]:

$$N_{\text{eff}} = N_{\nu} \left[ 1 + \frac{1}{N_{\nu}} \sum_{i=\psi,X} \frac{g_i}{2} F \left( \frac{m_i}{T_{\nu,D}} \right) \right]^{4/3}, \quad (3.12)$$

where  $g_{\psi} = 4$  (including antiparticles),  $g_X = 3$  and the function  $F$  is given by

$$F(x) = \frac{30}{7\pi^4} \int_x^{\infty} dy \frac{(4y^2 - x^2) \sqrt{y^2 - x^2}}{e^y \pm 1}; \quad (3.13)$$

the sign  $+$ ( $-$ ) refers to fermion (boson) statistics.  $F$  basically describes the entropy carried by a species of massive particle at  $T = T_{\nu,D}$ , which will then go into neutrinos, as explained above. The power  $4/3$  arises because we defined  $N_{\text{eff}}$  in eq.(3.11) via the energy density rather than via the entropy density; it is the energy density which determines the Hubble rate during BBN. We checked that this simplified treatment quite accurately reproduces numerical results in the literature [17, 38].

Numerical results for  $g_X = 5 \cdot 10^{-4}$  are shown in fig. 2. For large masses the contributions to  $N_{\text{eff}}$  vanish since then the decay or annihilation already happens at  $T > T_{\nu,D}$ , and thus goes into the overall SM plasma; this does not impact BBN, which happens at

---

<sup>2</sup>A leptonic asymmetry of the order of the baryon–antibaryon asymmetry is totally negligible for our purposes.

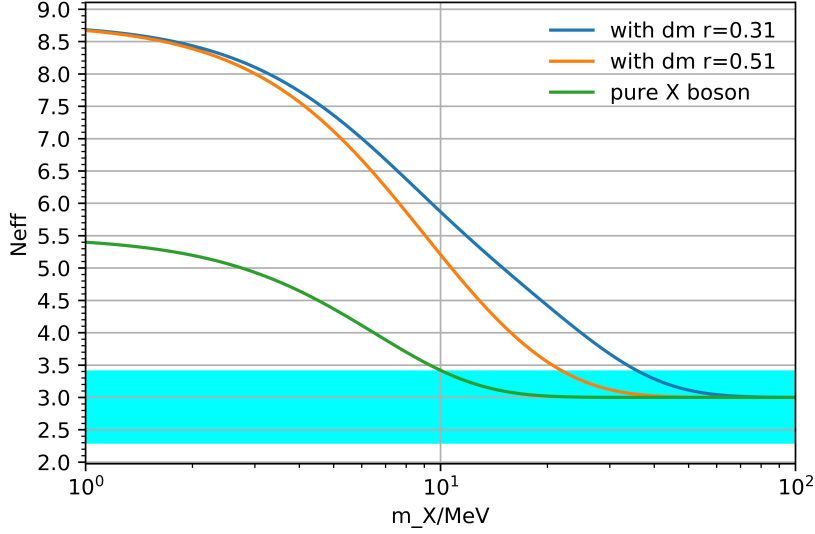


**Figure 2.** The contribution from  $X$  and  $\psi$  particles to  $N_{\text{eff}}$ , as function of  $m_X$  with  $m_\psi = r m_X$ . The lower (green) curve shows the contribution from  $X$  alone, while the orange and blue curves include the contribution from  $\psi\bar{\psi}$  annihilation with  $r = 0.51$  and  $0.31$ , respectively. The BBN allowed region [32] is shown in cyan.

temperatures well below  $T_{\nu,D}$ . In contrast, for masses  $\lesssim T_{\nu,D}$  the new particles would clearly increase  $N_{\text{eff}}$  well beyond the current bound; according to the Particle Data Group, successful BBN requires  $N_{\text{eff}} \leq 3.4$  at 95% confidence level. This imposes a lower bound on the relevant particle masses.

On the other hand, it has been shown [18, 19] that increasing  $N_{\text{eff}}$  somewhat above its SM value of 3.05 allows to alleviate the “Hubble tension”, i.e. the tension between the (low) value of today’s Hubble constant derived from anisotropies of the Cosmic Microwave Background (CMB) and other cosmological observations, and the (higher) value derived from direct, “local” measurements. We consider  $N_{\text{eff}} \geq 3.2$  as making a significant contribution to solving this puzzle.<sup>3</sup>

### 3.4 Cosmic Microwave Background

The CMB also gives a relevant limit on dark matter annihilation into charged particles after recombination [41, 42], which would increase the ionization fraction. This in turn would reduce the mean free path of CMB photons, which affects the pattern of CMB anisotropies. The resulting bound on the annihilation cross section is given by

$$f_{\text{eff}}(m_\psi) \frac{\langle \sigma v \rangle}{2} \leq 4.1 \times 10^{-28} \left( \frac{m_\psi}{\text{GeV}} \right) \text{cm}^3/\text{s}, \quad (3.14)$$

<sup>3</sup>The tension could be reduced even more if the neutrino free streaming length could be reduced below its SM value. However, this is only significant if the neutrino interaction strength at low energies,  $g_X^2/m_X^2$ , exceeds  $10^{-4}/\text{MeV}^2$  [19]; for  $m_X \sim 20$  MeV this would give much too large a contribution to  $g_\mu - 2$ .

where  $f_{\text{eff}}$  is an  $\mathcal{O}(1)$  parameter that describes the energy injection efficiency into ionization. This constraint applies to our model in two scenarios. If the dark matter mass is larger than the muon mass,  $\psi\bar{\psi} \rightarrow \mu\bar{\mu}$  becomes a main annihilation channel for dark matter, which determines its relic density. In this case, there is a lower bound on dark matter mass up to several GeV, which completely excludes the sub-GeV region for  $m_\mu < m_\psi$ .

If  $m_\psi \lesssim m_\mu$ , our dark matter particles dominantly annihilate into neutrinos, which have  $f_{\text{eff}} \sim 0$ . The bound (3.14) thus only applies to  $\psi\bar{\psi} \rightarrow e^+e^-$ , whose cross-section is  $\left(\frac{e\epsilon_A}{g_X}\right)^2 \approx 2 \times 10^{-5}$  smaller than that for  $\psi\bar{\psi} \rightarrow \nu\bar{\nu}$ . Nevertheless this constraint will play a role when we will try to explain the excess of 511 keV photons.

### 3.5 White Dwarf Cooling

White Dwarfs are created at very high temperatures. In the SM they cool by emitting photons and neutrinos, where the latter contribution is described by the standard weak interactions. The cooling rate can be constrained by observing the distributions of White Dwarfs as a function of their temperature or, equivalently, brightness. One finds that the SM prediction reproduces the observation fairly well. This can be used to constrain additional cooling mechanisms [43].

Neutrino emission contributes to cooling mostly through the “decay” of plasmon quasi-particles into  $\nu\bar{\nu}$  pairs. The rate for this process is proportional to the square of the effective coupling of neutrinos to the electron vector current. Since the  $Ze^+e^-$  coupling in the SM is mostly axial vector, in the SM the neutrino cooling is dominated by the emission of electron neutrinos, which also have charged current couplings to electrons. The corresponding effective Lagrangian can be written as

$$\mathcal{L}_{\text{eff,SM}} = -\frac{C_V G_F}{\sqrt{2}} (\bar{\nu}\gamma^\mu(1-\gamma_5)\nu)(\bar{e}\gamma_\mu e), \quad (3.15)$$

where  $G_F$  is the Fermi constant and  $C_V \simeq 1$  [43]. In the  $U(1)_{L_\mu-L_\tau}$  model there is an additional contribution to this effective Lagrangian, involving  $\mu$  and  $\tau$  neutrinos couplings to the electron current via eq.(2.2):

$$\delta\mathcal{L}_{\text{eff}} = -\frac{G_D}{2} q_l (\bar{\nu}_l\gamma^\mu(1-\gamma_5)\nu_l)(\bar{e}\gamma_\mu e), \quad (3.16)$$

with effective coupling

$$G_D = \frac{\epsilon_A g_X e}{m_X^2}; \quad (3.17)$$

here  $e$  is the QED coupling constant,  $\epsilon_A$  has been given in the second eq.(2.2), and  $q_l = 1$  ( $-1$ ) for  $l = \mu$  ( $\tau$ ).

In the SM, White Dwarf cooling by neutrino emission is important only at high temperatures. The constraint on this emission rate is therefore not very tight; according to ref. [43], the total neutrino emission rate should not exceed the SM prediction by more than a factor of 2. Taking into account that two generations of neutrinos contribute in eq.(3.16), this requires  $|G_D| \leq G_F$ , which in turn implies

$$\frac{g_X}{m_X} \leq 5.3 \cdot 10^{-4} \frac{10 \text{ MeV}}{m_X}. \quad (3.18)$$

The same interaction can be constrained [44] from the analysis of  $\nu e \rightarrow \nu e$  scattering, the most sensitive data coming from the Borexino collaboration [45]. According to [44, 46] the resulting bound is slightly weaker than that from White Dwarf cooling, so we do not show it.

### 3.6 Other Experimental Constraints

There is already a comprehensive study on how different experiments can constrain the parameter space of the  $U(1)_{L_\mu-L_\tau}$  model [44]. We therefore limit ourselves to a very brief discussion of the most relevant constraints, which are shown in fig. 3.

#### 3.6.1 Neutrino Trident Production

Neutrino trident production  $\nu_\mu N \rightarrow \nu_\mu N \mu^+ \mu^-$  has been shown to be a powerful tool to constrain the  $U(1)_{L_\mu-L_\tau}$  model [47]. It gives additional contributions via  $X$  exchange between the  $\nu_\mu$  and muon lines. The cross sections reported by the CHARM-II [48] and CCFR [49] collaborations are compatible with SM predictions and thus put strong limits on our model, as shown by the red line in fig. 3.

#### 3.6.2 Coherent Elastic Neutrino Nucleus Scattering

The coherent elastic neutrino nucleus scattering (CE $\nu$ NS) experiment constrains interactions between neutrinos and nuclei, i.e. up and down quarks [50]. Our  $U(1)_{L_\mu-L_\tau}$  model contributes to such process again via  $X$ -photon mixing, see eq.(2.2). Using data from scattering on both Cs and Ar nuclei one can derive a strong constraint on the parameter space; see the green curve in fig. 3.

#### 3.6.3 $X$ Production at BaBar

The BaBar experiment searched for spin-1 bosons which couple to muons via the process  $e^+e^- \rightarrow \mu^+\mu^-X$ ,  $X \rightarrow \mu^+\mu^-$  [51]. Note that they assume unit branching ratio for  $X \rightarrow \mu^+\mu^-$  decays; in our model this branching ratio never exceeds 50%. So the published bound should be interpreted as bound on  $g_X^2 \cdot \text{Br}(X \rightarrow \mu^+\mu^-)$ . The result is shown by the brown line in fig. 3.

### 3.7 Summary of the Allowed Parameter Space

The constraints discussed in this Section are summarized by fig. 3. The BBN constraint  $N_{\text{eff}} < 3.4$  requires  $m_X \gtrsim 20$  MeV, the precise value depending on the ratio  $m_\psi/m_X$ , as shown in fig. 2. On the other hand, the Hubble tension can be alleviated only for  $N_{\text{eff}} \geq 3.2$ , which requires  $m_X \lesssim 27$  MeV. These two constraints thus essentially fix the mass of the new gauge boson. The measurement of  $g_\mu - 2$  can then be used to determine the new gauge coupling  $g_X$ , as indicated by the light green region. Finally, the requirement that  $\psi$  has the correct thermal relic density in minimal cosmology determines  $m_\psi$ , or  $m_\psi/m_X$ , as shown in fig. 1.

So for a very restricted region of parameter space our model can already (help to) solve three puzzles: the existence of cosmological dark matter, the discrepancy between the SM prediction for and the measurement of  $g_\mu - 2$ , and the discrepancy between “cosmological”

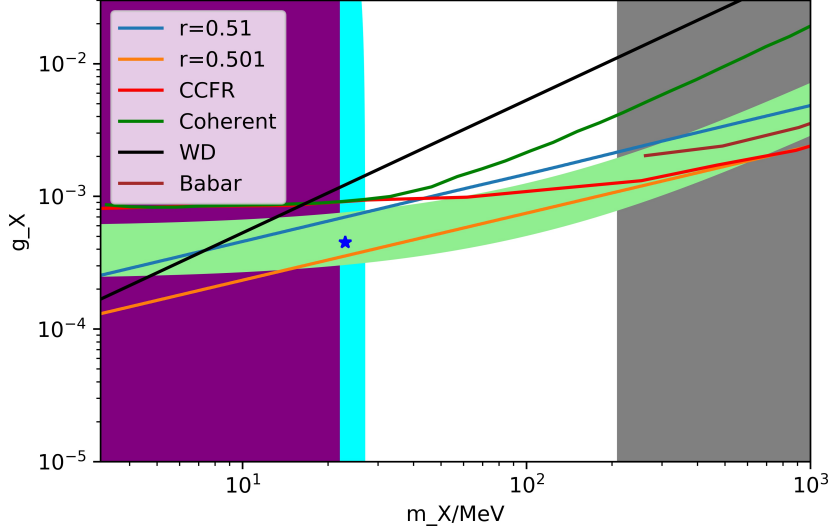


**Figure 3.** Parameter space of the  $U(1)_{L_\mu-L_\tau}$  model described by the gauge coupling  $g_X$  and the gauge boson mass  $m_X$ . The purple region is excluded by  $N_{\text{eff}}$ , the cyan region is favored by the Hubble tension, the gray region is excluded by the CMB, and the light green region allows to explain the measurement of  $g_\mu - 2$  within one standard deviation. The black, dark green, red, and brown lines are upper bounds on  $g_X$  from White Dwarf (WD) cooling, neutrino trident production (CCFR), neutrino nucleus coherent scattering, and the BaBar experiment. Parameters on the blue (orange) line reproduce the correct thermal relic dark matter density for  $m_\psi/m_X = 0.51$  (0.501) and charge  $q_\psi = 1$ . The blue star is the benchmark point used to study the 511 keV line.

and “local” measurements of the Hubble constant. We will now show that this model might explain yet another long-standing puzzle.

#### 4 511keV Line

Starting in the 1970’s a large flux of photons with energy of 511 keV from the center of our galaxy has been observed [20–24]. This sharp line can obviously be interpreted as originating from the annihilation of non-relativistic  $e^+e^-$  pairs. The challenge is to explain the rather high density of positrons required to reproduce the measurements.

It has been pointed out more than 15 years ago that dark matter annihilation into  $e^+e^-$  pairs could be responsible for this signal [52, 53]. This requires an annihilation cross section of

$$10^{-3}\text{fb} \leq \langle \sigma(\psi\bar{\psi} \rightarrow e^+e^-)v \rangle \cdot \left( \frac{m_\psi}{1 \text{ MeV}} \right)^{-2} / 2 \leq 1\text{fb} \quad (4.1)$$

for Dirac DM with  $n_\psi = n_{\bar{\psi}}$ ; the averaging is now over the DM velocity distribution in the region of the galactic center, where typically  $v \sim 10^{-3}$  (in natural units). Here we use the same conservative range as in [54], which is expanded by one order of magnitude compared with [53]. Note that the upper end of the range (4.1) is excluded by CMB constraints:

taking  $f_{\text{eff}}(10 \text{ MeV}) = 0.9$  [41], eq.(3.14) gives

$$\frac{\langle \sigma v \rangle}{2} \leq 0.015 \left( \frac{m_\psi}{1 \text{ MeV}} \right) \text{ fb}. \quad (4.2)$$

Since this bound depends linearly on the DM mass while the required cross-section grows quadratically with  $m_\psi$ ,<sup>4</sup> it prevents DM particles with mass above 15 MeV from explaining the 511 keV line. However, upper bounds on the flux of MeV photons from the galactic center in any case imply [55, 56]  $m_\psi < 3 \text{ MeV}$  if DM annihilation alone explains the positron flux. This stringent constraint can be relaxed by reducing the dark matter contribution. We estimate that the annihilation of 10 MeV DM particles can still contribute 30 to 40% of the 511 keV flux. The remainder would then have to originate from astrophysical processes producing at most mildly relativistic positrons; note that the upper bound of 3 MeV, which originates from positron annihilation in flight [56], really refers to the positron injection energy, which equals  $m_\psi$  for positrons from  $\psi\bar{\psi} \rightarrow e^+e^-$  annihilation.

Recall that the DM coupling to  $e^+e^-$  is loop suppressed in our model; the cross section for annihilation into  $e^+e^-$  pairs can thus be estimated as

$$\langle \sigma(\psi\bar{\psi} \rightarrow e^+e^-)v \rangle \approx \left( \frac{e}{70} \right)^2 \langle \sigma(\psi\bar{\psi} \rightarrow \nu\bar{\nu})v \rangle \approx 2 \times 10^{-5} \langle \sigma(\psi\bar{\psi} \rightarrow \nu\bar{\nu})v \rangle. \quad (4.3)$$

In the non-relativistic limit appropriate for DM annihilation in today's universe the cross section of eq.(2.3) can be simplified. Using

$$s \approx 4m_\psi^2 + m_\psi^2 v_{\text{rel}}^2, \quad (4.4)$$

where  $v_{\text{rel}}$  denotes the relative velocity between annihilating DM particles in the center-of-mass frame, and defining

$$r = m_\psi/m_X; \quad \delta = 4r^2 - 1; \quad \gamma_X = \Gamma_X/m_X, \quad (4.5)$$

the annihilation cross section can be written as

$$\sigma(\psi\bar{\psi} \rightarrow \nu_l\bar{\nu}_l)v \approx \frac{q_\psi^2 g_X^4}{8\pi m_X^2} \frac{1}{(\delta + v_{\text{rel}}^2/4)^2 + \gamma_X^2}. \quad (4.6)$$

Due to the loop suppression in eq.(4.3) we need today's  $\psi\bar{\psi}$  annihilation cross section to be significantly larger than that at decoupling if DM annihilation is to contribute significantly to the positron flux. As explained at the end of Sec. 3.1 we thus need  $r$  to be slightly larger than 0.5, so that the cross section is Breit-Wigner enhanced with an unphysical pole [57, 58]. The enhancement of today's averaged annihilation cross section over that at decoupling is called the “boost factor” (BF); it is determined by  $\delta$  and  $\gamma_X$ :

$$\text{BF} = \frac{\max[\delta, \gamma_X]^{-1}}{10}. \quad (4.7)$$

---

<sup>4</sup>The difference comes about because the CMB restricts the *energy* injected in form of  $e^+e^-$  pairs, whereas the flux of 511 keV photons is proportional to the *number* of such pairs.

In the interesting region of parameter space  $\gamma_X \sim 10^{-8}$  is always much smaller than  $\delta$ . For  $r > 0.5$  we need an averaged DM annihilation cross at decoupling of about 1 pb<sup>5</sup>; this corresponds to  $v_{\text{rel}}^2/4 \simeq 0.1$ . Today  $v_{\text{rel}}^2/4 \lesssim 10^{-6}$  in our galaxy; for  $\delta > 10^{-6}$  today's averaged cross section is then approximately given by

$$\langle\sigma v\rangle_{\text{now}} \approx \frac{\delta^{-1}}{10} \text{ pb}. \quad (4.8)$$

Of course,  $\delta$  cannot be chosen arbitrarily; as we saw in Sec. 3.1, it is determined by the requirement that the DM relic density comes out right. In our previous analysis we had set the DM charge  $q_\psi = 1$ . A smaller DM charge will force the DM mass to be closer to the pole, giving a smaller value of  $\delta$ . We can therefore increase today's annihilation cross section into  $e^+e^-$  pairs by reducing  $q_\psi$ ; of course, we still need to take care not to violate the CMB constraint.

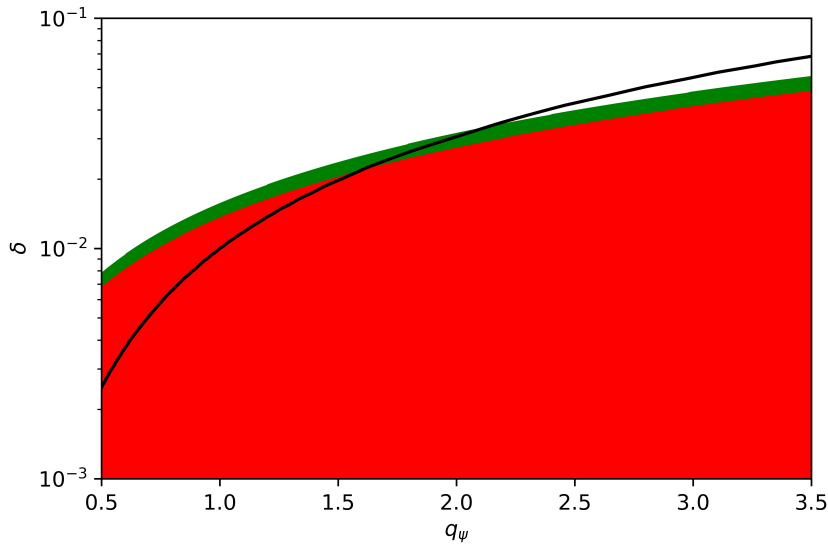


**Figure 4.** The parameter space spanned by DM charge  $q_\psi$  and  $\delta = 4m_\psi^2/m_X^2 - 1$ , for gauge coupling  $g_X = 4.5 \times 10^{-4}$  and  $m_X = 23$  MeV. On the black line the thermal relic density in minimal cosmology has the desired value. In the green region DM annihilation might explain the 511 keV line, while the red region is excluded by the CMB constraint (4.2).

Fig. 4 shows numerical results in the  $q_\psi - \delta$  plane. We see that DM annihilation in our model might explain the excess of 511 keV photons if  $1.5 \lesssim q_\psi \lesssim 2.2$ <sup>6</sup>; for even smaller values of  $q_\psi$  the cross section for annihilation into  $e^+e^-$  pairs violates the CMB constraint (4.2). Due this constraint DM annihilation can probably produce a sizable contribution to

<sup>5</sup>For  $r < 0.5$ ,  $\langle\sigma v\rangle$  at decoupling actually needs to be closer to 50 pb, because in that case  $\langle\sigma v\rangle$  drops very quickly with increasing  $x$ , reducing the annihilation integral  $J$ ; this effect would also make DM annihilation in today's universe unobservable for  $r < 0.5$ .

<sup>6</sup>This range is quite sensitive to gauge coupling  $g_X$ : for  $g_X = 5.4 \cdot 10^{-4}$ ,  $1.1 \lesssim q_\psi \lesssim 1.5$  is preferred while for  $g_X = 3.2 \cdot 10^{-4}$ ,  $3.1 \lesssim q_\psi \lesssim 4.1$  is needed. These values bracket the  $2\sigma$  range of  $g_\mu - 2$ .

the required positron flux only if the DM density peaks rather strongly close to the galactic center. Note also that the constraints shown in Fig. 3 do not depend on  $q_\psi$ . The DM charge thus offers a handle to tune the contribution to the flux of 511 keV photons from DM annihilation.

## 5 Future Tests

Future tests of this model have also been discussed in ref. [44]. We therefore limit ourselves to two remarks.

First, for parameters that allow to explain the 511 keV line, the discussion of the previous Section shows that our model predicts a large annihilation cross section into neutrinos in today's universe,  $\langle\sigma(\psi\bar{\psi} \rightarrow \nu_l\bar{\nu}_l)v\rangle_{\text{now}} \approx 10^{-24} - 10^{-25} \text{ cm}^3/\text{s}$ . According to estimates in [59] the corresponding flux of neutrinos with  $E_\nu = m_\psi \simeq 10 \text{ MeV}$  should be easily detectable at next generation neutrino experiments like JUNO [60] through neutrino–electron scattering.

Secondly, in the entire range  $m_X \lesssim 200 \text{ MeV}$  where the model can simultaneously produce a good thermal DM candidate and explain the measurement of  $g_\mu - 2$  without violating existing constraints, it might also be testable through the process  $e^+e^- \rightarrow X\gamma$  followed by invisible decays of the  $X$  boson [54]. The differential cross section reads:

$$\frac{d\sigma}{d\cos\theta} = \frac{\alpha(e\epsilon_A)^2}{s(s-m_X^2)} \left[ \frac{s^2 + m_X^4}{\sin^2\theta} - \frac{(s-m_X^2)^2}{2} \right], \quad (5.1)$$

where  $\alpha$  is the fine structure constant and  $\theta$  is the angle between the photon and the beam direction in the center-of-mass frame. Requiring  $|\cos\theta| < 0.985$  in order to make sure that the photon can be detected and taking  $m_X^2 \ll s$  leads to a cross section of about

$$\sigma \simeq 20\text{ab} \left( \frac{g_X}{10^{-3}} \right)^2 \frac{(10 \text{ GeV})^2}{s}. \quad (5.2)$$

The signature is a photon with center of mass energy  $E_\gamma = (s-m_X^2)/(2\sqrt{s}) \simeq \sqrt{s}/2$ , without any other detectable particles. This has very little physics background from  $e^+e^- \rightarrow \nu\bar{\nu}\gamma$ , the cross section for which scales like  $\alpha G_F^2 s$ . Currently the  $B$ -factory Belle-II operates at  $\sqrt{s} \simeq 10 \text{ GeV}$ ; its goal is to achieve an integrated luminosity of  $50 \text{ ab}^{-1}$  [61], leading to hundreds of signal events for  $g_X = 5 \cdot 10^{-4}$ . Similarly, the proposed super tau–charm factory in China would operate at  $\sqrt{s} \simeq 4 \text{ GeV}$  with integrated luminosity around  $2 \text{ ab}^{-1}$  per year; this would yield a similar number of signal events with even less physics background.

## 6 Summary and Conclusions

In this paper we showed that the  $U(1)_{L_\mu-L_\tau}$  model with a Dirac dark matter particle  $\psi$  can be used to explain four different observations. The measurement of  $g_\mu - 2$ , which exceeds the SM prediction by 4.2 standard deviations, can be explained through the exchange of the new light gauge boson  $X$  for  $U(1)_{L_\mu-L_\tau}$  coupling  $g_X \simeq 5 \cdot 10^{-4}$ . For this value of  $g_X$  the thermal dark matter relic density comes out correct for DM charge  $q_\psi \simeq 1$  if  $m_\psi \simeq m_X/3$  or if  $m_\psi$

is just above  $m_X/2$ . Moreover, if  $m_X \simeq 20$  MeV the decoupling of  $X$  and  $\psi$  increases the radiation content of the universe by  $\delta N_{\text{eff}} \lesssim 0.4$ , which respects BBN constraints but allows to alleviate the tension between cosmological and “local” measurements of the Hubble constant. Finally, for the same range of  $m_X$  and  $m_\psi$  just above  $m_X/2$ ,  $\psi\bar{\psi} \rightarrow e^+e^-$  annihilation might help to explain the excess of 511 keV photons from the center of our galaxy. This part of parameter space is compatible with all other experimental and astrophysical constraints. Moreover, there are two other, less well established, observations which might prefer this scenario over the SM: our  $X$  boson will slightly speed up the cooling of hot White Dwarfs via the emission of  $\nu_\mu$  and  $\nu_\tau$  pairs; according to ref. [62] there is indeed some evidence for additional White Dwarf cooling (which is interpreted in terms of axion emission in that work). Secondly, this range of  $m_X$  also appears to be slightly favored by IceCube 6 years shower data relative to the SM-only hypothesis [63].

As discussed in ref. [44] this model can be tested in future beam dump experiments. We point out that the entire parameter range that can explain both  $g_\mu - 2$  and the DM relic density should be testable through single photon searches at super flavor factories. This requires the implementation of a single photon trigger; we urge our experimental colleagues in the BELLE-II collaboration, as well as those working on the design of detectors for future tau-charm factories, to consider this. Moreover, the choice of parameters that allows to explain the excess of 511 keV photons leads to a large flux of  $\nu_\mu$  and  $\nu_\tau$  with energy  $E_\nu = m_\psi \simeq 10$  MeV, which should be detectable by future neutrino experiments like DUNE.

### Acknowledgments:

We thank John Beacom for bringing ref.[56] to our attention.

**Note added:** In the final stages of our work ref. [64] appeared, which has considerable overlap with this work. Our results in general agree with their’s. However, they do not discuss white dwarf constraints, the 511 keV excess, and possible signals at low-energy  $e^+e^-$  colliders.

### References

- [1] X.G. He, G.C. Joshi, H. Lew and R.R. Volkas, *New Z-prime Phenomenology*, *Phys. Rev. D* **43** (1991) 22.
- [2] P. Fayet, *U-boson production in  $e^+e^-$  annihilations,  $\psi$  and Upsilon decays, and Light Dark Matter*, *Phys. Rev. D* **75** (2007) 115017 [[hep-ph/0702176](#)].
- [3] M. Pospelov, *Secluded  $U(1)$  below the weak scale*, *Phys. Rev. D* **80** (2009) 095002 [[0811.1030](#)].
- [4] MUON G-2 collaboration, *Measurement of the Positive Muon Anomalous Magnetic Moment to 0.46 ppm*, *Phys. Rev. Lett.* **126** (2021) 141801 [[2104.03281](#)].
- [5] T. Aoyama et al., *The anomalous magnetic moment of the muon in the Standard Model*, *Phys. Rept.* **887** (2020) 1 [[2006.04822](#)].

- [6] S. Baek, *Dark matter and muon  $(g - 2)$  in local  $U(1)_{L_\mu-L_\tau}$ -extended Ma Model*, *Phys. Lett. B* **756** (2016) 1 [[1510.02168](#)].
- [7] S. Patra, S. Rao, N. Sahoo and N. Sahu, *Gauged  $U(1)_{L_\mu-L_\tau}$  model in light of muon  $g - 2$  anomaly, neutrino mass and dark matter phenomenology*, *Nucl. Phys. B* **917** (2017) 317 [[1607.04046](#)].
- [8] A. Biswas, S. Choubey and S. Khan, *Neutrino Mass, Dark Matter and Anomalous Magnetic Moment of Muon in a  $U(1)_{L_\mu-L_\tau}$  Model*, *JHEP* **09** (2016) 147 [[1608.04194](#)].
- [9] A. Kamada, K. Kaneta, K. Yanagi and H.-B. Yu, *Self-interacting dark matter and muon  $g - 2$  in a gauged  $U(1)_{L_\mu-L_\tau}$  model*, *JHEP* **06** (2018) 117 [[1805.00651](#)].
- [10] M. Drees, M. Shi and Z. Zhang, *Constraints on  $U(1)_{L_\mu-L_\tau}$  from LHC Data*, *Phys. Lett. B* **791** (2019) 130 [[1811.12446](#)].
- [11] E.J. Chun, A. Das, J. Kim and J. Kim, *Searching for flavored gauge bosons*, *JHEP* **02** (2019) 093 [[1811.04320](#)].
- [12] Y. Kahn, G. Krnjaic, N. Tran and A. Whitbeck,  *$M^3$ : a new muon missing momentum experiment to probe  $(g - 2)_\mu$  and dark matter at Fermilab*, *JHEP* **09** (2018) 153 [[1804.03144](#)].
- [13] R. Garani and J. Heeck, *Dark matter interactions with muons in neutron stars*, *Phys. Rev. D* **100** (2019) 035039 [[1906.10145](#)].
- [14] P. Foldenauer, *Light dark matter in a gauged  $U(1)_{L_\mu-L_\tau}$  model*, *Phys. Rev. D* **99** (2019) 035007 [[1808.03647](#)].
- [15] K. Asai, S. Okawa and K. Tsumura, *Search for  $U(1)_{L_\mu-L_\tau}$  charged Dark Matter with neutrino telescope*, *JHEP* **03** (2021) 047 [[2011.03165](#)].
- [16] N. Okada and O. Seto, *Inelastic extra  $U(1)$  charged scalar dark matter*, *Phys. Rev. D* **101** (2020) 023522 [[1908.09277](#)].
- [17] M. Escudero, D. Hooper, G. Krnjaic and M. Pierre, *Cosmology with A Very Light  $L_\mu - L_\tau$  Gauge Boson*, *JHEP* **03** (2019) 071 [[1901.02010](#)].
- [18] S. Vagnozzi, *New physics in light of the  $H_0$  tension: An alternative view*, *Phys. Rev. D* **102** (2020) 023518 [[1907.07569](#)].
- [19] E. Di Valentino, O. Mena, S. Pan, L. Visinelli, W. Yang, A. Melchiorri et al., *In the realm of the Hubble tension—a review of solutions*, *Class. Quant. Grav.* **38** (2021) 153001 [[2103.01183](#)].
- [20] I. Johnson, W. N., J. Harnden, F. R. and R.C. Haymes, *The Spectrum of Low-Energy Gamma Radiation from the Galactic-Center Region.*, *Astrophysical Journal* **172** (1972) L1.
- [21] R.C. Haymes, G.D. Walraven, C.A. Meegan, R.D. Hall, F.T. Djuth and D.H. Shelton, *Detection of nuclear gamma rays from the galactic center region.*, *Astrophysical Journal* **201** (1975) 593.
- [22] M. Leventhal, C.J. MacCallum and P.D. Stang, *Detection of 511 keV positron annihilation radiation from the galactic center direction.*, *Astrophysical Journal* **225** (1978) L11.
- [23] J. Knodlseder et al., *Early SPI / INTEGRAL constraints on the morphology of the 511 keV line emission in the 4th galactic quadrant*, *Astron. Astrophys.* **411** (2003) L457 [[astro-ph/0309442](#)].

- [24] C.A. Kierans et al., *Detection of the 511 keV Galactic Positron Annihilation Line with COSI*, *Astrophys. J.* **895** (2020) 44 [[1912.00110](#)].
- [25] K. Asai, *Predictions for the neutrino parameters in the minimal model extended by linear combination of  $U(1)_{L_e-L_\mu}$ ,  $U(1)_{L_\mu-L_\tau}$  and  $U(1)_{B-L}$  gauge symmetries*, *Eur. Phys. J. C* **80** (2020) 76 [[1907.04042](#)].
- [26] K. Asai, K. Hamaguchi, N. Nagata, S.-Y. Tseng and K. Tsumura, *Minimal Gauged  $U(1)_{L_\alpha-L_\beta}$  Models Driven into a Corner*, *Phys. Rev. D* **99** (2019) 055029 [[1811.07571](#)].
- [27] K. Asai, K. Hamaguchi and N. Nagata, *Predictions for the neutrino parameters in the minimal gauged  $U(1)_{L_\mu-L_\tau}$  model*, *Eur. Phys. J. C* **77** (2017) 763 [[1705.00419](#)].
- [28] MUON G-2 collaboration, *Final Report of the Muon E821 Anomalous Magnetic Moment Measurement at BNL*, *Phys. Rev. D* **73** (2006) 072003 [[hep-ex/0602035](#)].
- [29] K. Griest and D. Seckel, *Three exceptions in the calculation of relic abundances*, *Phys. Rev. D* **43** (1991) 3191.
- [30] F. Ambrogio, C. Arina, M. Backovic, J. Heisig, F. Maltoni, L. Mantani et al., *MadDM v.3.0: a Comprehensive Tool for Dark Matter Studies*, *Phys. Dark Univ.* **24** (2019) 100249 [[1804.00044](#)].
- [31] P. Gondolo and G. Gelmini, *Cosmic abundances of stable particles: Improved analysis*, *Nuclear Physics B* **360** (1991) 145.
- [32] PARTICLE DATA GROUP collaboration, *Review of Particle Physics*, *PTEP* **2020** (2020) 083C01.
- [33] R. Essig, M. Fernandez-Serra, J. Mardon, A. Soto, T. Volansky and T.-T. Yu, *Direct Detection of sub-GeV Dark Matter with Semiconductor Targets*, *JHEP* **05** (2016) 046 [[1509.01598](#)].
- [34] R. Essig, A. Manalaysay, J. Mardon, P. Sorensen and T. Volansky, *First Direct Detection Limits on sub-GeV Dark Matter from XENON10*, *Phys. Rev. Lett.* **109** (2012) 021301 [[1206.2644](#)].
- [35] XENON collaboration, *Light Dark Matter Search with Ionization Signals in XENON1T*, *Phys. Rev. Lett.* **123** (2019) 251801 [[1907.11485](#)].
- [36] DARKSIDE collaboration, *Constraints on Sub-GeV Dark-Matter–Electron Scattering from the DarkSide-50 Experiment*, *Phys. Rev. Lett.* **121** (2018) 111303 [[1802.06998](#)].
- [37] SENSEI collaboration, *SENSEI: Direct-Detection Results on sub-GeV Dark Matter from a New Skipper-CCD*, *Phys. Rev. Lett.* **125** (2020) 171802 [[2004.11378](#)].
- [38] A. Kamada, K. Kaneta, K. Yanagi and H.-B. Yu, *Self-interacting dark matter and muon  $g-2$  in a gauged  $U(1)_{L_\mu-L_\tau}$  model*, *JHEP* **06** (2018) 117 [[1805.00651](#)].
- [39] K.M. Nollett and G. Steigman, *BBN And The CMB Constrain Neutrino Coupled Light WIMPs*, *Phys. Rev. D* **91** (2015) 083505 [[1411.6005](#)].
- [40] C. Boehm, M.J. Dolan and C. McCabe, *A Lower Bound on the Mass of Cold Thermal Dark Matter from Planck*, *JCAP* **08** (2013) 041 [[1303.6270](#)].
- [41] T.R. Slatyer, *Indirect dark matter signatures in the cosmic dark ages. I. Generalizing the bound on s-wave dark matter annihilation from Planck results*, *Phys. Rev. D* **93** (2016) 023527 [[1506.03811](#)].

- [42] R.K. Leane, T.R. Slatyer, J.F. Beacom and K.C.Y. Ng, *GeV-scale thermal WIMPs: Not even slightly ruled out*, *Phys. Rev. D* **98** (2018) 023016 [[1805.10305](#)].
- [43] H.K. Dreiner, J.-F. Fortin, J. Isern and L. Ubaldi, *White Dwarfs constrain Dark Forces*, *Phys. Rev. D* **88** (2013) 043517 [[1303.7232](#)].
- [44] M. Bauer, P. Foldenauer and J. Jaeckel, *Hunting All the Hidden Photons*, *JHEP* **07** (2018) 094 [[1803.05466](#)].
- [45] G. Bellini et al., *Precision measurement of the  $^7\text{Be}$  solar neutrino interaction rate in Borexino*, *Phys. Rev. Lett.* **107** (2011) 141302 [[1104.1816](#)].
- [46] Y. Kaneta and T. Shimomura, *On the possibility of a search for the  $L_\mu - L_\tau$  gauge boson at Belle-II and neutrino beam experiments*, *PTEP* **2017** (2017) 053B04 [[1701.00156](#)].
- [47] W. Altmannshofer, S. Gori, M. Pospelov and I. Yavin, *Neutrino Trident Production: A Powerful Probe of New Physics with Neutrino Beams*, *Phys. Rev. Lett.* **113** (2014) 091801 [[1406.2332](#)].
- [48] D. Geiregat et al., *First observation of neutrino trident production*, *Physics Letters B* **245** (1990) 271.
- [49] S. Mishra et al., *Neutrino trident and  $w$ - $z$  interference*, *Phys. Rev. Lett.* **66** (1991) 3117.
- [50] M. Cadeddu, N. Cargioli, F. Dordei, C. Giunti, Y.F. Li, E. Picciani et al., *Constraints on light vector mediators through coherent elastic neutrino nucleus scattering data from COHERENT*, *JHEP* **01** (2021) 116 [[2008.05022](#)].
- [51] BABAR collaboration, *Search for a muonic dark force at BABAR*, *Phys. Rev. D* **94** (2016) 011102 [[1606.03501](#)].
- [52] C. Boehm and Y. Ascasibar, *More evidence in favor of light dark matter particles?*, *Phys. Rev. D* **70** (2004) 115013.
- [53] C. Boehm, D. Hooper, J. Silk, M. Casse and J. Paul, *MeV dark matter: Has it been detected?*, *Phys. Rev. Lett.* **92** (2004) 101301 [[astro-ph/0309686](#)].
- [54] N. Borodatchenkova, D. Choudhury and M. Drees, *Probing MeV dark matter at low-energy  $e^+e^-$  colliders*, *Phys. Rev. Lett.* **96** (2006) 141802 [[hep-ph/0510147](#)].
- [55] J.F. Beacom, N.F. Bell and G. Bertone, *Gamma-ray constraint on Galactic positron production by MeV dark matter*, *Phys. Rev. Lett.* **94** (2005) 171301 [[astro-ph/0409403](#)].
- [56] J.F. Beacom and H. Yuksel, *Stringent constraint on galactic positron production*, *Phys. Rev. Lett.* **97** (2006) 071102 [[astro-ph/0512411](#)].
- [57] M. Ibe, H. Murayama and T.T. Yanagida, *Breit-Wigner Enhancement of Dark Matter Annihilation*, *Phys. Rev. D* **79** (2009) 095009 [[0812.0072](#)].
- [58] M. Ibe, Y. Nakayama, H. Murayama and T.T. Yanagida, *Nambu-Goldstone Dark Matter and Cosmic Ray Electron and Positron Excess*, *JHEP* **04** (2009) 087 [[0902.2914](#)].
- [59] C.A. Argüelles, A. Diaz, A. Kheirandish, A. Olivares-Del-Campo, I. Safa and A.C. Vincent, *Dark Matter Annihilation to Neutrinos*, [1912.09486](#).
- [60] JUNO collaboration, *Neutrino Physics with JUNO*, *J. Phys. G* **43** (2016) 030401 [[1507.05613](#)].
- [61] BELLE-II collaboration, *Belle II Technical Design Report*, [1011.0352](#).

- [62] J. Isern, E. Garcia-Berro, S. Torres, R. Cojocaru and S. Catalan, *Axions and the luminosity function of white dwarfs: the thin and thick discs, and the halo*, *Mon. Not. Roy. Astron. Soc.* **478** (2018) 2569 [[1805.00135](#)].
- [63] J.A. Carpio, K. Murase, I.M. Shoemaker and Z. Tabrizi, *High-energy cosmic neutrinos as a probe of the vector mediator scenario in light of the muon  $g - 2$  anomaly and Hubble tension*, [2104.15136](#).
- [64] I. Holst, D. Hooper and G. Krnjaic, *The Simplest and Most Predictive Model of Muon  $g - 2$  and Thermal Dark Matter*, [2107.09067](#).